



## Young uplift in the non-glaciated parts of the Eastern Alps

Thomas Wagner <sup>a,\*</sup>, Derek Fabel <sup>b</sup>, Markus Fiebig <sup>c</sup>, Philipp Häuselmann <sup>d</sup>, Diana Sahy <sup>c,1</sup>, Sheng Xu <sup>e</sup>, Kurt Stüwe <sup>a</sup>

<sup>a</sup> Institute of Earth Sciences, Karl-Franzens University, Universitätsplatz 2, 8010, Graz, Austria

<sup>b</sup> Department of Geographical and Earth Sciences, University of Glasgow, G12 8QQ, Scotland, UK

<sup>c</sup> Institute of Applied Geology, Department of Civil Engineering and Natural Hazards, University of Natural Resources and Applied Life Sciences, Peter Jordan Strasse 70, 1190, Vienna, Austria

<sup>d</sup> Swiss Institute for Speleology and Karst Studies, La Chaux-de-Fonds, 2301, Switzerland

<sup>e</sup> Scottish Universities Environmental Research Centre (SUERC), Rankine Avenue, Scottish Enterprise Technology Park, East Kilbride, G75 0QF, Scotland, UK

### ARTICLE INFO

#### Article history:

Received 2 December 2009

Received in revised form 12 March 2010

Accepted 22 March 2010

Editor: T.M. Harrison

#### Keywords:

burial age  
cosmogenic nuclides  
caves  
river incision  
landscape evolution

### ABSTRACT

We report the first incision rates derived from burial ages of cave sediments from the Mur river catchment at the eastern margin of the Eastern Alps. At the transition zone between the Alpine orogen and the Pannonian basin, this river passes through the Paleozoic of Graz – a region of karstifiable rocks called the Central Styrian Karst. This river dissects the study area in a north–south direction and has left behind an abundance of caves. These caves can be grouped into several distinct levels according to their elevation above the present fluvial base level. Age estimates of abandoned cave levels are constrained by dating fluvial sediments washed into caves during the waning stages of speleogenesis with the terrestrial cosmogenic nuclide method. These ages and the elevations of the cave levels relative to the current valley floor are used to infer a very complex history of 4 million years of water table position, influenced by the entrenchment and aggradation of the Mur river. We observe rather low rates of bedrock incision over the last 4 Ma (in the order of 0.1 mm/y) with an e-folding decrease in this trend to lower rates at younger times. We relate this incision history to a tectonic setting where an increase of drainage area of the Mur river due to stream piracy in Late Miocene to Pliocene times is linked to surface uplift. The later decrease in valley lowering rates is attributed to the rise of the base level related to aggradation of sediments within the valley. Sediment transport through the valley from the upstream section of the Mur river limited the erosional potential of the river to a transport limited state at the later stages of the incision history.

© 2010 Elsevier B.V. All rights reserved.

### 1. Introduction

The young tectonic evolution of the Alps is a much debated topic in Earth science. Many studies investigate the uplift history and landscape evolution of the range over the last 10 Ma employing low temperature geochronological methods (Dunkl et al., 2005; Luth and Willingshofer, 2008; Vernon et al., 2008), geodetic uplift measurements (Kahle et al., 1997; Ruess and Höggerl, 2002), the interpretation of morphometric data (Frisch et al., 2001; Robl et al., 2008; Székely et al., 2002) and new cosmogenic isotope methods to measure erosion rates (von Blanckenburg, 2005; Wittmann et al., 2007; Norton et al., 2010).

Much of this debate focuses on the central Alps where it has been argued that the range is past its peak of tectonic activity and acts now merely in passive response to erosion (Champagnac et al., 2009; Schlunegger and Hinderer, 2001), despite its dramatic topography of up to 4000 m of relief. In contrast, the eastern margin of the Alps currently appears to experience a tectonic rejuvenation: Miocene fission track ages (e.g. Hejl, 1997) and post-Middle Miocene sediment cover (Dunkl and Frisch, 2002) suggest that much of the Neogene evolution of the eastern margin of the orogen was likely to be characterised by little relief and low elevation and that – therefore – today's topography is rather young. Morphological evidence for this is provided by paleosurfaces at higher elevations and steeply dissected gorges with an obvious break in slopes at about 1000 m a.s.l. (above sea level) in a landscape with up to 2000 m relief (Winkler-Hermaden, 1957).

This scenario – and the difference between the central and the eastern Alps – is consistent with our understanding of the plate scale tectonic processes: The rotation pole of the Adriatic plate is currently located near Torino south of the central Alps suggesting tectonic quiescence in the central Alps, but ongoing north–south convergence in the east (Champagnac et al., 2009; Fodor et al., 2005; Grenerczy

\* Corresponding author. Tel.: +43 316 380 5680; fax: +43 316 380 9865.

E-mail addresses: [thomas.wagner@uni-graz.at](mailto:thomas.wagner@uni-graz.at) (T. Wagner), [derek.fabel@ges.gla.ac.uk](mailto:derek.fabel@ges.gla.ac.uk) (D. Fabel), [markus.fiebig@boku.ac.at](mailto:markus.fiebig@boku.ac.at) (M. Fiebig), [praezis@speleo.ch](mailto:praezis@speleo.ch) (P. Häuselmann), [diyh@bgs.ac.uk](mailto:diyh@bgs.ac.uk) (D. Sahy), [s.xu@suerc.gla.ac.uk](mailto:s.xu@suerc.gla.ac.uk) (S. Xu), [kurt.stuewe@uni-graz.at](mailto:kurt.stuewe@uni-graz.at) (K. Stüwe).

<sup>1</sup> Present address: Department of Geology, University of Leicester & NERC Isotope Geosciences Laboratory, British Geological Survey, Keyworth, Nottingham, NG12 5GG, UK.

et al., 2000, 2005). Moreover, general consensus holds that the inversion of the Pannonian basin commenced in response to the cessation of subduction underneath the Carpathian arc and ongoing north–south convergence became the dominant stress regime in the area since then (Bada et al., 2007; Horváth and Cloething, 1996; Ruszkiczay-Rüdiger, 2007). Onset of uplift in the Styrian Basin (being the western most lobe of the Pannonian Basin) around Pliocene to Quaternary times (Sachsenhofer et al., 1997) appears to be a reflection of this process. Moreover, mantle processes like slab break off or delamination may influence uplift rates (e.g. Genser et al., 2007).

Interestingly, specific data sets documenting this uplift are almost absent. In this paper we present cosmogenically derived burial ages of sediments from caves within the karstifiable rocks of the Paleozoic of Graz as the first evidence for a young incision history of the major drainage system that drains the Alps to the East: the Mur system. We show that the incision of this system is slow but acts on a rejuvenating setting, providing an exciting illustration of the revitalization of a landscape forming process: a juvenile stage of relief adjustment to changes in rock uplift rates.

## 2. Topography of the eastern margin

The eastern margin of the Alps is the only part of the Eastern Alps that was never ice covered during the Quaternary (Fig. 1A; Van Husen, 1999). As such, glacial carving can be excluded as a land forming process and the region is uniquely suited to infer the pre-Quaternary uplift history from the incision history of its drainages.

In very general terms, the drainage system of the Eastern Alps evolved in relation to the eastward extrusion of the range (Frisch et al., 1998; Ratschbacher et al., 1991). Of the three major eastward

draining rivers, the Enns-Salzach system in the north and the Drava system in the south follow major west–east striking strike slip systems. The third major drainage, the Mur, roots from the highest peaks of the eastern Alps at an elevation of 1898 m a.s.l. and drains much of the central region of the range eastwards into the Pannonian basin. In contrast to the others, the Mur does not follow any major fault system downstream of Bruck (Fig. 1A). Morphological analysis of these three major drainage systems shows that the Enns-Salzach and the Drava systems have knickpoints in their main channels that can be correlated with glacial features, while the Mur – outside the glaciated region – has an equilibrium channel profile (Robl et al., 2008). However, a complicated set of stream terraces above the channel indicates that the river had a complicated aggradation and incision history (Winkler-Hermaden, 1955, 1957). Nevertheless, because of (i) the absence of fault control of the lower Mur; (ii) the fact that the Mur crosses the (Alpine) orogen–(Pannonian) basin transition near the city of Graz and (iii) the fortuitous fact that this transition zone is made up of karstified rocks, we focus here on dating the incision history of the Mur drainage system.

### 2.1. Caves as a proxy for landscape evolution

The drainage basin of the Mur above Radkersburg is some 10000 km<sup>2</sup> in area and its main channel has a total length of 295 km from its spring down to the Austrian border. The so-called Central Styrian Karst, located at the orogen basin transition zone, belongs tectonically to the Paleozoic of Graz. Its most intensively karstified region consists of Upper Devonian limestones. As the Paleozoic of Graz is only some tens of kilometers across and only partly made up of limestones (Fig. 1B), many caves are recharged

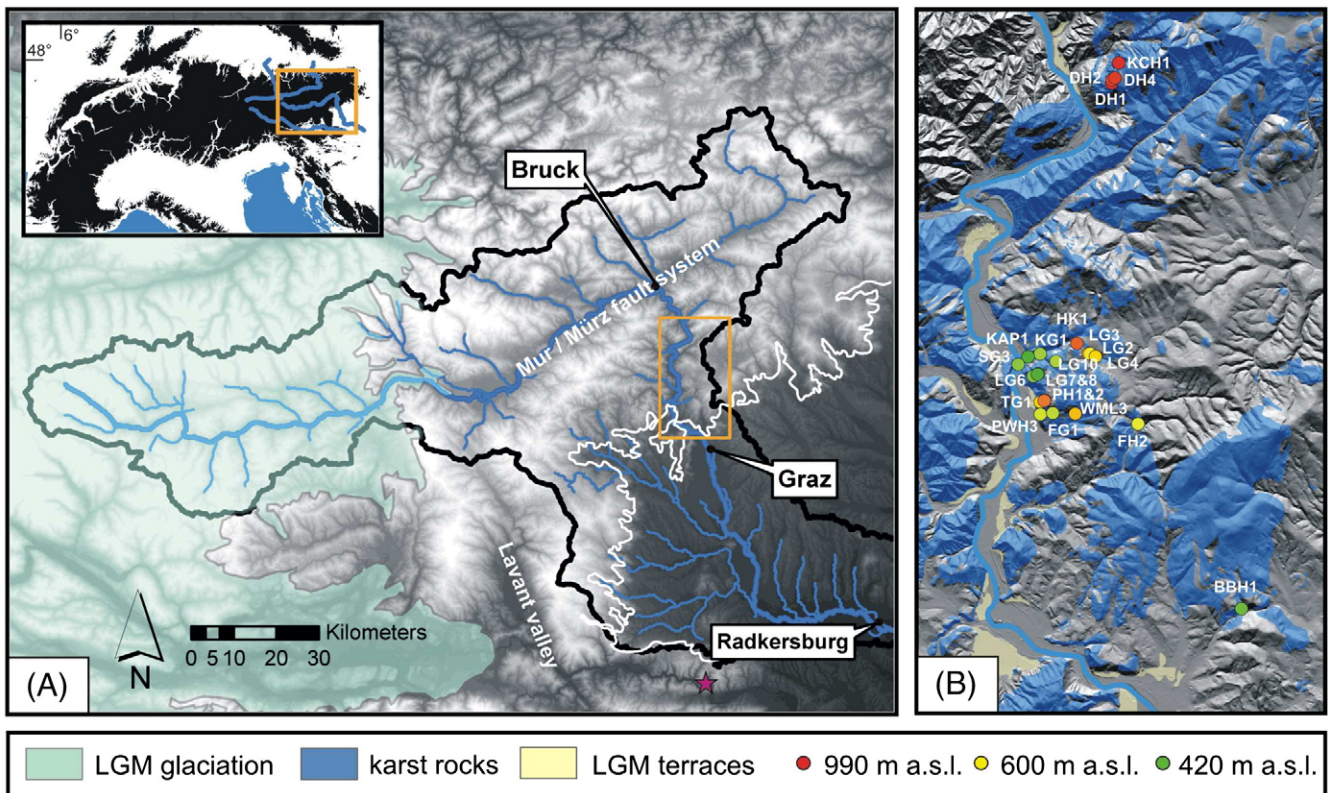


**Fig. 1.** Map showing the geographical position of the area under investigation. (A) The extend of the last glacial maximum in light blue, the perimeter of the Mur catchment as a black line, the orogen-basin transition as a white line and in blue the main river and larger tributaries displayed on top of the digital elevation model (white above 2000 m a.s.l., darkest shades about 200 m a.s.l.). The orange rectangle shows the area enlarged in 1B. The star indicates the site of an exposure age dated sample along the Drava river. The inset shows the whole Alps with an elevation above 600 m a.s.l. in black, indicating the area under investigation situated at the easternmost end of the Eastern Alps. Blue lines show the major rivers in the Eastern Alps. (B) Karstifiable rocks in blue and the last glacial terraces in yellow on top of a digital elevation model. Dots show the sample locations of the various cave sediments color coded according to their elevations above sea level (red = highest, green = lowest). Labeling of sample acronyms as used in Table 1.

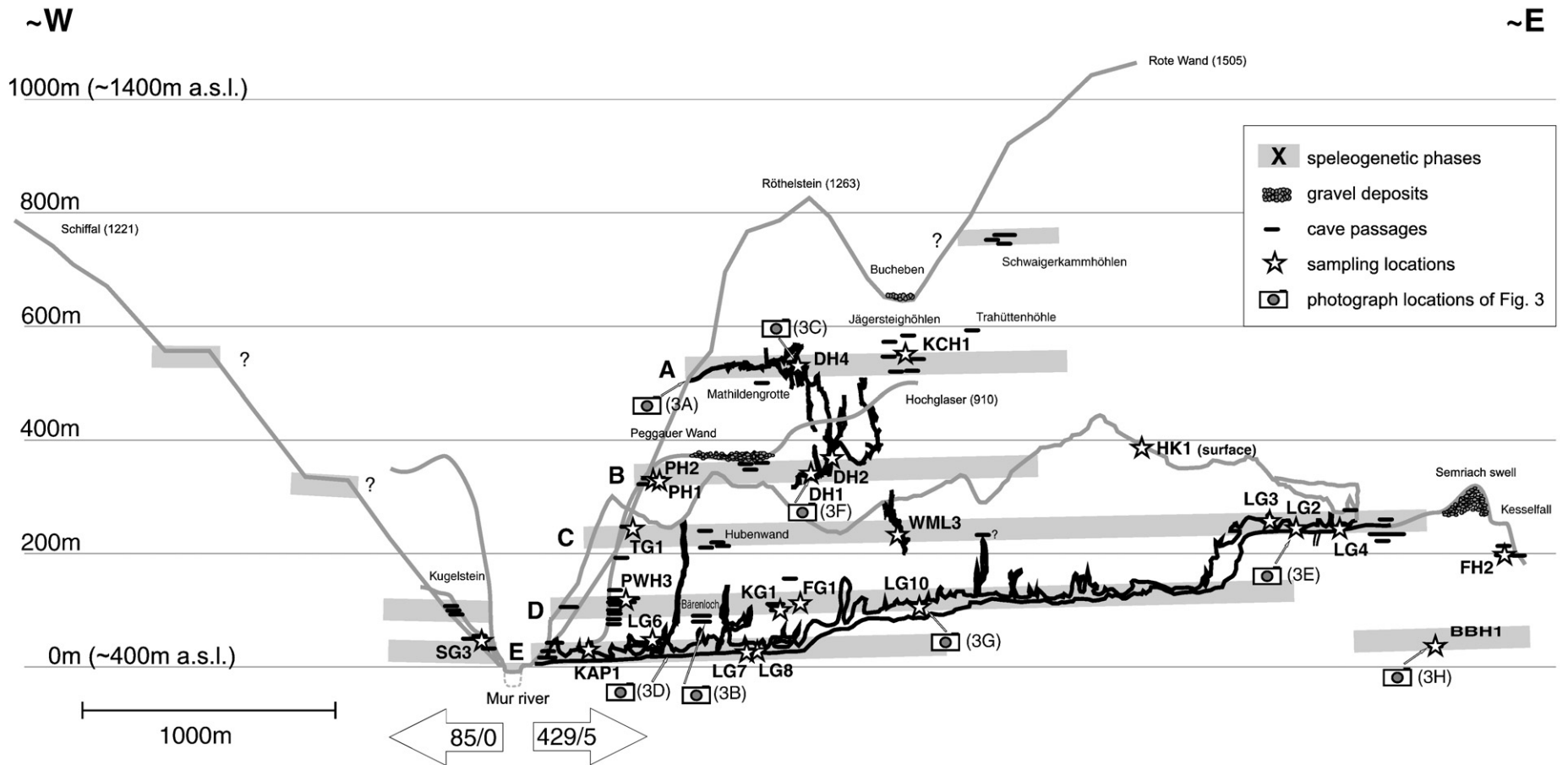


**Fig. 2.** Projected schematic view of cave systems of the Central Styrian Karst. Smaller caves illustrated by small black horizontal bars. Subhorizontal grey bars show speleogenetic phases A–E inferred from abundance of phreatic cave passages at these elevations. Stars indicate sampling locations of dated cave sediments. Camera symbols indicate the positions of the photographs shown in Fig. 3. Elevation in meters above the modern Mur river. Note that the whole region shows an asymmetrical distribution of dissolution caves and gravel deposits (see Section 2.1). Sample acronyms correspond to the following caves: Tanneben massif: FG = Ferdinandsgrotte, KAP = Kapellenhöhle, KG = Keesgang/Große Badlhöhle, LG = Lurgrotte, PH = Percohöhle, PWH = Peggauerwandhöhle, SG = Stufengrotte, TG = Tausgrotte, WML = Wildemannloch; Hochlantsch area: DH = Drachenhöhle, KCH = Kuschcanon; FH = Frauenhöhle, BBH = Blaubruchhöhle.

from siliceous rocks in the upland. Because of this and the fact that the topographic relief within and outside the Paleozoic of Graz is similar, local variations in incision and erosion rates are unlikely to be the consequence of differences in lithology. Caves are concentrated in two areas, the Hochlantsch area in the north and the Tanneben massif further south (Fig. 1B). Geologically, the Hochlantsch area is located in the upper whereas the Tanneben is in the lower nappe system of the Paleozoic of Graz (Fig. 1B). In the Hochlantsch area higher cave levels are preserved, whereas in the Tanneben massif most of these have been eroded (Gasser et al., 2009). A total of some 500 caves that range from active caves on the current base level of the Mur to inactive caves up to about 800 m above the current valley floor are recorded in the Austrian cave registry. Caves are typically of phreatic origin with occasional vadose overprint (Fig. 3H). Sub-horizontal tubular passages are widespread and can be grouped into at least 5 distinguishable cave levels, or speleogenetic phases (Fig. 2). In the caves, we interpret these levels as indicators for the position of the former water table. They correlate well with other morphological features like terraces and planation surfaces across the region (Maurin and Benischke, 1992; Winkler-Hermaden, 1957). However, for this study we focus on caves alone because of (i) their abundance, (ii) because of the preservation of sediments within the caves and (iii) because surface markers are so far undated.

As erosion lowers the valley floor, the water table drops, leaving the caves as a record for the elevation of the paleo-water table (according to the concept of base level control of cave levels; Palmer, 1987). Many of the caves contain allochthonous sediments of fluvial origin made up of quartzose sand and coarse gravels derived from the crystalline hinterland and interpreted to be deposited during the waning stages of passage formation (Fig. 3). However, we will show later that they are likely to have been derived from sources within the close vicinity of the karstified region. As such they are ideally not influenced by further upstream sections of the main (Mur) river. The vertical distance between cave levels can be used to infer relative incision rates if the time of passage formation is known. Here we constrain the minimum age of passages by dating the time of emplacement of allochthonous quartzous fluvial sediments into the cave and interpret these ages as the time when valley incision progressed to abandon the passage level. Consequently, the calculated incision rates represent maximum values.

Field mapping demonstrates an asymmetrical distribution of caves and gravel accumulations along the Mur valley. An abundance of caves is observed on the eastern river side and scarcity on the western as sketched on Fig. 2. The Austrian cave registry lists 429 known caves on the eastern, but only 85 on the western river side. The five largest cave systems are all found on the eastern river side. A satisfying explanation for this is the focus of ongoing research and therefore of a speculative nature, but it is considered likely that it might be related to a westward shift of the Mur river (e.g. Maurin and Benischke, 1992). This observation illustrates the complexity of the study area.

The main focus of our study are the Lurgrotte located in the Tanneben area and the Drachenhöhle (Fig. 3A) in the Hochlantsch area. These are two of the largest cave systems of the Styrian Karst, and both exhibit more than one level or speleogenetic phase. The Lurgrotte is the longest cave system in the Tanneben area (5975 m, 273 m vertical extent) and is developed along three subhorizontal levels (levels C–E, Fig. 2). Only the lower level is permanently active, but passages situated at higher elevations show obvious signs of reactivation, for example sinking streams during flood events (e.g. as shown by organic sedimentation within the cave). The whole cave system was filled with sediments and re-excavated several times,

even in historical records. In the Hochlantsch area, the Drachenhöhle (length 4386 m, depth 250 m) shows two obvious speleogenetic phases developed along strike of bedding in the Hochlantsch limestones (Fig. 2). The upper level, here defined as level A, is situated at about 950 to 1000 m a.s.l., while the lower level of the Drachenhöhle can be correlated with the highest caves found in the Tanneben massif (level B) based on its elevation above streambed. Lower karstified levels, corresponding to levels C–E from the Tanneben massif, are less developed in the Hochlantsch region and did not contain sediments suitable for dating (Fig. 3B). Smaller caves from the Hochlantsch and Tanneben areas were correlated to distinct levels of the Drachenhöhle, and the Lurgrotte, respectively; based on similar elevation above the modern valley floor. In total, this speleogenetic record allows us to infer paleo-water table lowering over a vertical extent of more than 550 m.

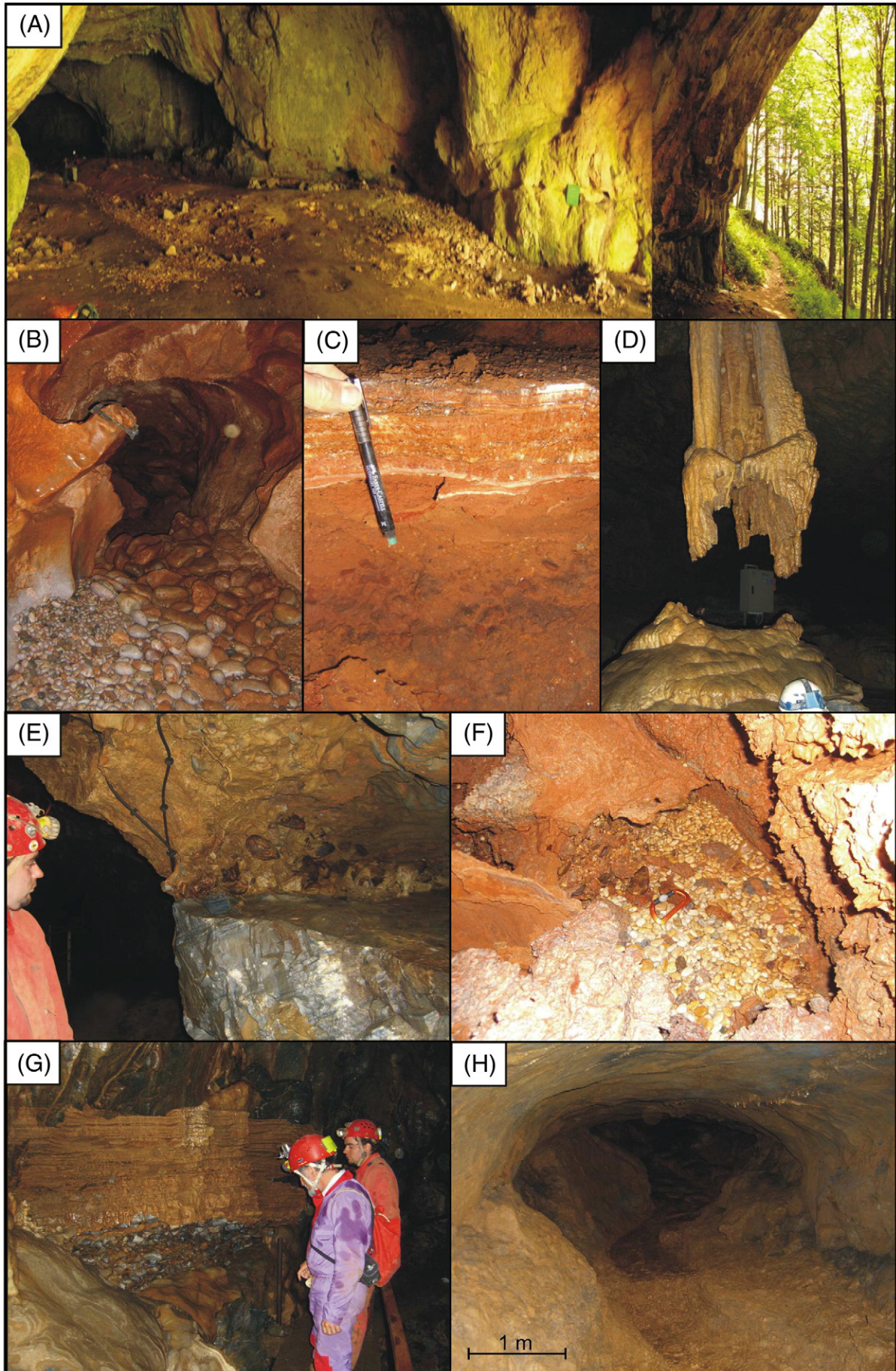
A total of more than 120 caves have been investigated spanning a vertical range of 780 m. Finally, we selected 13 caves and dated 22 samples comprising siliceous rock pebbles (fine to very coarse gravels) using cosmogenic isotopes (for sample locations see Fig. 1B and Fig. 2). Careful subsurface field mapping was used to ascertain that the sampled sediments represent characteristic stages of passage formation. Additionally, one surface sample (HK1) was dated using cosmogenic isotopes to test for the presence of inherited burial signal in samples collected in the caves. Targeted U–Th dating of speleothems was used to support the burial ages with independent ages from stratigraphically related sediments (Table 2 and Fig. 3C, G).

### 3. Burial ages

Deriving burial ages from cave sediments is a relatively new method (Granger et al., 2001) not yet successfully applied in the Eastern Alps (first attempts by Frisch et al., 2001). It involves the measurement of two isotopes (here  $^{26}\text{Al}$  and  $^{10}\text{Be}$ ) that are produced by cosmic radiation in quartz near the surface prior to burial.  $^{26}\text{Al}$  and  $^{10}\text{Be}$  accumulate at a ratio of about 6.8:1 in quartz grains – a few atoms per gram of quartz per year. Quick and deep burial of such quartz-rich sediment in a cave (>20 m rock overburden) assures shielding from further cosmic rays. After burial the  $^{26}\text{Al}$  and  $^{10}\text{Be}$  concentrations in the sample are only affected by their relative decay resulting in a decrease in the  $^{26}\text{Al}/^{10}\text{Be}$  ratio in the samples. Measured  $^{26}\text{Al}/^{10}\text{Be}$  in the samples can be used to derive a burial age (Gosse and Phillips, 2001; Granger and Muzikar, 2001). The current upper limit for measurement of the  $^{26}\text{Al}$  and  $^{10}\text{Be}$  isotope pair is around 5 my. A prerequisite of the burial dating technique is that samples have been exposed long enough to cosmic rays and accumulated sufficient cosmogenic nuclides prior to burial. Unfortunately this cannot be determined a priori in the field.

In the laboratory, about 100 g of quartz was extracted and purified from bulk samples by magnetic and density separation and selective chemical dissolution. Quartz was dissolved in a 5:1 solution of concentrated HF and  $\text{HNO}_3$  and spiked with about 0.74 mg  $^9\text{Be}$ . Al and Be were separated and purified by ion chromatography and selective precipitation. Precipitates were oxidized and mixed with metal powder for accelerator mass spectrometry (AMS).  $^{10}\text{Be}/^9\text{Be}$  and  $^{26}\text{Al}/^{27}\text{Al}$  nuclide ratios in the sample and procedural blanks were measured at the SUERC AMS facility in Glasgow. The procedural blanks yielded  $^{10}\text{Be}/^9\text{Be}$  ratios  $<3.6 \times 10^{-15}$  and  $^{26}\text{Al}/^{27}\text{Al}$  ratios of  $<2.5 \times 10^{-15}$ , representing <6% of total  $^{10}\text{Be}$  atoms and <10% of total  $^{26}\text{Al}$  atoms in the samples. Only sample TG1 had low measured ratios of  $11.5 \pm 0.9 \times 10^{-15}$  and  $5.4 \pm 1.8 \times 10^{-15}$  respectively and the procedural blanks represent <22% and <46% of the

**Fig. 3.** Field impressions from the Central Styrian Karst: (A) Portal of the Drachenhöhle, Hochlantsch area. (B) Active passage of the Bärenloch, Hochlantsch area. Note that all the well rounded pebbles are carbonate rock only. (C) Sample location of sample DH4: Gravels as well as flowstone were dated (see Tables 1 and 2). (D) The so-called Prinz (prince) at level E of the Lurgrotte, an impressive stalagmite with gravel remainings at its base indicating former aggradation of this passage. (E) Sample location of sample LG2 in a wall notch at level C of the Lurgrotte. (F) Sample location of sample DH1 at the lower level B of the Drachenhöhle. (G) Sample location of sample LG10: Further entrenchment of the gallery has left behind remnants of an impressive calcite false floor with gravel remains still attached below indicating an aggradation event of level D in the Lurgrotte. (H) Phreatic passage in the Blaubruchhöhle showing the typical elliptic tube with beginning vadose overprint (key hole).



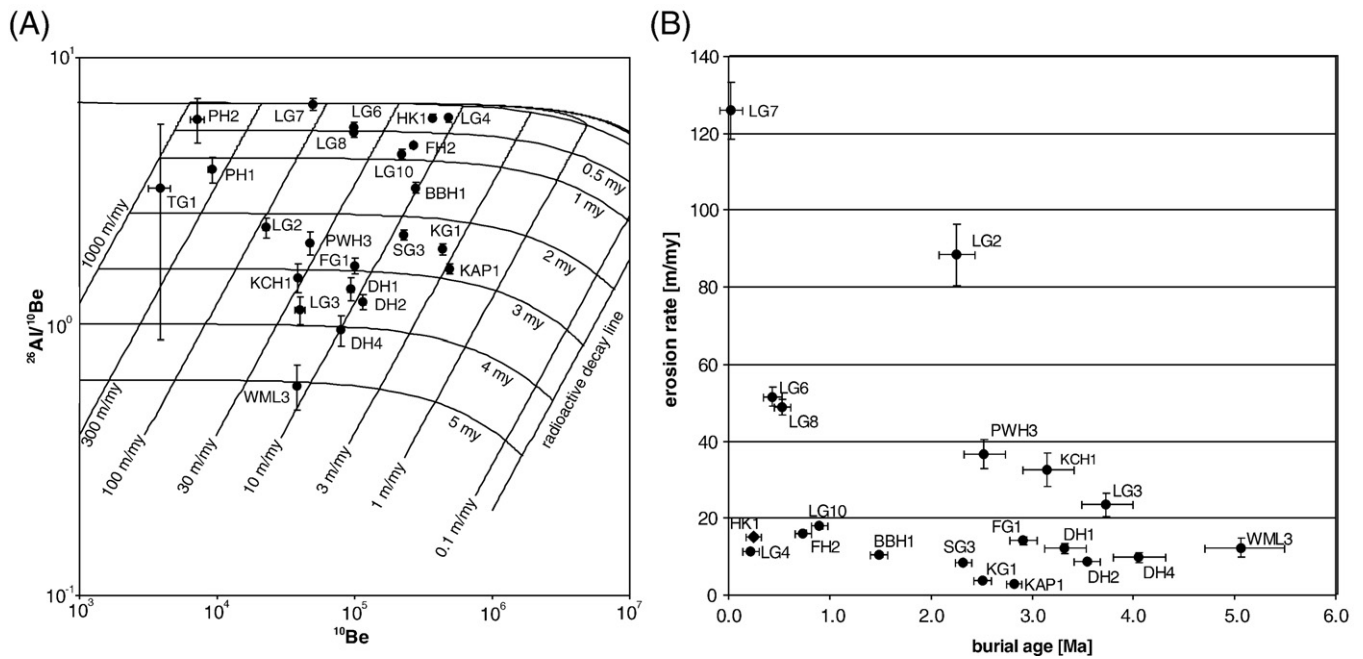


**Fig. 4.** Burial age data graphically displayed. (A) Two isotope plot showing the samples burial ages and pre-burial erosion rates, assuming local production rates as shown in Table 1. (B) Burial age versus pre-burial erosion rates, suggesting rather constant erosion rates in the source areas of the cave sediments of about 20 m/my. TG1, PH1 and PH2 are outside the plotted range (see Section 3).

$^{10}\text{Be}$  and  $^{26}\text{Al}$  atoms respectively. Stable aluminium concentrations were determined by ICP-OES. The stated errors are  $1\sigma$  calculated from AMS and ICP-OES uncertainties. Aside from obtaining burial age data, the isotope concentrations can also be used to infer paleo-erosion rates of the source

area prior to burial of the clasts. This is accomplished by backward modeling the quantity of nuclides present prior to the burial coupled with local production rate estimates. Cosmogenic nuclide production rates were assumed to be constant and were estimated for a mean source

**Table 1**  
Cosmogenic nuclide concentrations and sediment burial ages from caves in the Central Styrian Karst.

Sample	A.C.R. No.	Height*** (m)	$^{26}\text{Al}^*$ ( $10^4$ at/g)	$^{10}\text{Be}^*$ ( $10^4$ at/g)	$^{26}\text{Al}/^{10}\text{Be}$	Burial age** (Ma)	Erosion rate# (m/my)
LG7	2836/1	25 ± 5	33.37 ± 1.33	4.98 ± 0.19	6.70 ± 0.37	0.02 ± 0.12	125.95 ± 7.41
KAP1	2836/19	25 ± 5	80.54 ± 2.44	49.19 ± 1.53	1.64 ± 0.07	2.82 ± 0.09	2.77 ± 0.13
LG8	2836/1	26.5 ± 5	51.81 ± 1.43	9.87 ± 0.26	5.25 ± 0.20	0.53 ± 0.08	48.86 ± 2.00
BBH1	2832/3	34 ± 5	90.79 ± 2.84	27.70 ± 0.90	3.28 ± 0.15	1.48 ± 0.09	10.47 ± 0.51
LG6 <sup>§</sup>	2836/1	45 ± 5	54.07 ± 0.96	9.83 ± 0.39	5.50 ± 0.24	0.43 ± 0.09	51.60 ± 2.40
SG3	2784/6	47 ± 5	49.65 ± 1.08	22.66 ± 0.81	2.19 ± 0.09	2.32 ± 0.09	8.30 ± 0.38
LG10 <sup>§</sup>	2836/1	91 ± 5	95.77 ± 1.97	21.94 ± 0.79	4.36 ± 0.18	0.90 ± 0.09	18.01 ± 0.81
KG1	2836/17	100 ± 5	84.67 ± 2.57	43.71 ± 1.56	1.94 ± 0.09	2.51 ± 0.09	3.75 ± 0.19
FG1	2836/44	107 ± 5	16.77 ± 0.96	9.98 ± 0.35	1.68 ± 0.11	2.91 ± 0.14	14.17 ± 1.03
PWH3	2836/38	117 ± 5	9.71 ± 0.88	4.76 ± 0.19	2.04 ± 0.20	2.52 ± 0.22	36.66 ± 3.93
FH2	2832/15	205 ± 5	125.32 ± 2.47	26.61 ± 0.95	4.71 ± 0.19	0.74 ± 0.09	16.11 ± 0.71
WML3	2836/27	225 ± 5	2.30 ± 0.42	3.81 ± 0.16	0.60 ± 0.11	5.06 ± 0.43	12.33 ± 2.51
LG2	2836/1	243 ± 5	5.30 ± 0.35	2.28 ± 0.12	2.33 ± 0.20	2.25 ± 0.19	88.38 ± 8.03
LG4	2836/1	245 ± 5	288.97 ± 5.64	48.36 ± 1.57	5.98 ± 0.23	0.22 ± 0.08	11.46 ± 0.47
TG1	2836/82	245 ± 5	1.27 ± 0.89	0.39 ± 0.07	3.27 ± 2.38	1.54 ± 2.74	750.01 ± 600.60
LG3	2836/1	260 ± 5	4.59 ± 0.42	4.00 ± 0.31	1.15 ± 0.14	3.73 ± 0.27	23.44 ± 3.06
PH1	2836/164	325 ± 5	3.53 ± 0.29	0.92 ± 0.06	3.83 ± 0.41	1.20 ± 0.24	372.93 ± 43.45
PH2	2836/164	331 ± 5	4.26 ± 0.64	0.72 ± 0.08	5.91 ± 1.11	0.29 ± 0.44	759.55 ± 154.23
DH1	2839/1	350 ± 5	12.99 ± 1.12	9.41 ± 0.48	1.38 ± 0.14	3.31 ± 0.22	12.17 ± 1.32
DH2	2839/1	370 ± 5	14.15 ± 0.72	11.50 ± 0.46	1.23 ± 0.08	3.54 ± 0.14	8.79 ± 0.62
HK1	-	385 ± 5	216.87 ± 3.33	36.55 ± 1.18	5.93 ± 0.21	0.25 ± 0.08	15.04 ± 0.58
DH4 <sup>§</sup>	2839/1	528 ± 5	7.74 ± 0.94	7.97 ± 0.29	0.97 ± 0.12	4.05 ± 0.28	9.83 ± 1.36
KCH1	2839/37	550 ± 5	5.88 ± 0.68	3.88 ± 0.17	1.51 ± 0.19	3.15 ± 0.27	32.60 ± 4.34

\*  $^{26}\text{Al}/^{27}\text{Al}$  and  $^{10}\text{Be}/^{9}\text{Be}$  measured by accelerator mass spectrometry at the SUERC AMS facility relative to Z92-0222 with  $^{26}\text{Al}/^{27}\text{Al}$  taken as  $4.11 \times 10^{-11}$  and NIST SRM 4325 with  $^{10}\text{Be}/^{9}\text{Be}$  taken as  $3.06 \times 10^{-11}$ .  $\sim 0.74$  mg  $^9\text{Be}$  added as carrier to  $\sim 100$  g quartz samples. Quartz [Al] measured by ICP-OES (PerkinElmer, Optima 5300 DV) and assigned 3% uncertainty.

\*\* Burial ages and erosion rates determined by iterative solution of Eqs. (14) and (15) in Granger and Muzikar (2001), assuming local production rates of  $P_{n\&t,26} = 74.1$  at  $\text{g}^{-1} \text{yr}^{-1}$  and  $P_{n\&t,10} = 10.9$  at  $\text{g}^{-1} \text{yr}^{-1}$ , based on the CRONUS Earth online calculator (Version 2.2). Reported uncertainties represent  $1\sigma$  measurement uncertainty. For comparing the burial ages this is sufficient, but when comparing them with other burial ages, total uncertainties including systematic uncertainties in production rates,  $^{26}\text{Al}/^{10}\text{Be}$  production ratio and radioactive decay constants would have to be taken into account.

\*\*\* Height of the sample sites is given in meters above the current fluvial base level of the Mur river.

# Modeled pre-burial erosion rates of the source area of the cave sediments prior to burial assuming local production rates of  $P_{n\&t,26} = 74.1$  at  $\text{g}^{-1} \text{yr}^{-1}$  and  $P_{n\&t,10} = 10.9$  at  $\text{g}^{-1} \text{yr}^{-1}$ , based on the CRONUS Earth online calculator (Version 2.2). For discussion see Section 3 – Burial ages.

§ Burial ages are supported by speleothem U-series ages. The age estimates of stratigraphically related speleothems are considerably younger than the burial ages of the gravels, which is consistent with the conclusions of Stock et al. (2005a).

**Table 2**

U–Th age estimates of stratigraphically related speleothems from caves in the Central Styrian Karst. Sample preparation and measurements done by John Hellstrom, University of Melbourne. Activity ratios were determined with a Nu Plasma MC-ICP-MS following the procedure of Hellstrom (2003). Age is corrected for initial  $^{230}\text{Th}$  using Eq. (1) of Hellstrom (2006) and an initial  $[^{230}\text{Th}/^{232}\text{Th}]$  of  $1.5 \pm 1.5$  (uncertainties are fully propagated). 95% confidence intervals of the last digits of each value are given within round brackets.

Sample	Lab no.	U ( $\text{ngg}^{-1}$ )	$[^{230}\text{Th}/^{238}\text{U}]$	$[^{234}\text{U}/^{238}\text{U}]$	$[^{232}\text{Th}/^{238}\text{U}]$	$[^{230}\text{Th}/^{232}\text{Th}]$	Age (ka)	$[^{234}\text{U}/^{238}\text{U}]_i$
LG6-FSB	UMA02795 Jul-2009	104	1.081(5)	1.688(5)	0.02254(24)	1.9	$99.6 \pm 2.1$	1.913(7)
LG10-FSB	UMA02796 Jul-2009	80	1.285(7)	1.736(4)	0.29751(169)	2.1	$99.9 \pm 32.3$	1.977(88)
DH4-FSB	UMA02793 Jul-2009	72	1.113(10)	1.084(4)	0.22907(162)	1.4	$559(+\text{inf}/-110)$	$1.427(+0.53/-\text{inf})$

altitude of 1000 m a.s.l. and a latitude of  $47.2^\circ$ . While we cannot exclude variations in the elevation of the source area over the last few millions of years, we consider our estimate of 1000 m to be realistic. The pre-burial  $^{26}\text{Al}/^{10}\text{Be}$  ratio ( $\sim 6.8:1$ ) is basically not influenced by production rate and thus elevation (Nishiizumi et al., 1989; Stock et al., 2005b) and therefore burial ages remain unaffected by altitude changes in the source area. However, our assumption increases the uncertainty of our pre-burial erosion rates, as these are based on measured isotope concentrations and elevation dependant production rates.

Fig. 4A shows our results in a logarithmic two isotope plot. The curved lines are burial ages in million years; the steep straight lines are radioactive decay trajectories plotted for pre-burial erosion rates (m/my) increasing from right to left. It can be seen that the measured burial ages range from practically zero to 5 Ma, spanning the whole range of the burial age dating method (Fig. 4A). Some samples experienced only minor burial: the Lurgrotte samples LG7 and LG4 and the surface sample HK1. The Lurgrotte samples LG4 and LG7 were taken from flood deposits close to the current active streams in the cave at level E and C which explains their young age. Sample HK1 was collected at the surface on top of the Tanneben massif at 780 m a.s.l. and has a finite burial age of  $0.25 \pm 0.08$  Ma indicating that other samples may also have experienced a minor but complex burial history prior to their deposition in the caves. The fact that the dating method yielded young ages at sites where subsurface mapping indicated the possibility of late emplacement of the sediments increases the overall confidence level of the dataset. Complementary to this, all the U–Th ages of stratigraphically related speleothems are significantly younger than the burial ages of subjacent gravels (Tables 1 and 2).

Some samples show relatively high pre-burial erosion rates above 300 m/my (PH1, PH2 and TG1; Fig. 4). Interestingly, all these samples come from caves located in a prominent gully of the Tanneben massif, where field work indicates that late deposition of sediments into caves is possible. Moreover, the high pre-burial erosion rates indicate possibly strong erosion events around the time of sediment deposition in the cave. This implies that the burial ages of these samples may not necessarily reflect a meaningful age of passage formation. Most of the other samples give pre-burial erosion rates around 20 m/my (Fig. 4B). These rather consistent and low pre-burial erosion rates over the whole time span support the fact that strong changes in erosion rates in the system either by tectonics or by climate are unlikely in the local catchments. Among these samples, there is a corresponding correlation of burial age and elevation with a noticeable clustering of data around 2.5 Ma.

### 3.1. Interpretation of the data in terms of incision

Plotting the burial age data from Fig. 4 against sample elevation above the current Mur level provides insight into the landscape evolution of the region (Fig. 5). In the ideal case such a presentation of the data should reflect the abandoning of formerly phreatic passages and lowering of the paleo-water table, which can ultimately be used to infer the rate of valley entrenchment (Audra et al., 2006). The surface sample HK1 and the samples LG4 and LG7 (documented above to belong to recent deposits/events) are not shown on Fig. 5. The oldest burial age for each level is used as it corresponds to the minimum age of passage formation if re-mobilization from higher levels can be excluded (Häuselmann and Granger, 2005). Fig. 5 shows that the study area has a more complex history. First of all it must be noted that our data stem not from a single cave system, but from an abundance of smaller cave systems and remnants thereof. Because of this and because of the complex aggradation and incision history of the region all obtained ages must be discussed individually before any trends can be interpreted.

The group of samples with low ages and high elevations on Fig. 5 has been discussed above: Except for FH2 they are all samples with high pre-burial erosion rates (Fig. 4) and are explained by later emplacement of the gravels. Sample FH2 comes from a cave in an independent limestone area that was influenced by another speleogenetic base level. Field observations show that this base level only incised 60 m (in the dated 0.75 Ma) since the cave was abandoned. In Fig. 5 it appears higher, because the vertical axis shows elevation above the Mur. If it were plotted only 60 m above the Mur, its age is consistent with others at that elevation above their respective trunk streams. The oldest burial age, sample WML3, comes from a shaft cave on the Tanneben massif, where there is evidence for complex multiphase formation. The sample was collected above massive terra rossa deposits interpreted by Maurin and Benischke (1992) as evidence for a Quaternary warm period in the region. This would indicate reversed stratigraphy and demands the exclusion of this data point from the incision rate estimation. However its burial age of  $5.06 \pm 0.43$  Ma indicates the existence of older (and higher) cave levels in the Tanneben area that are no longer preserved. Finally, KCH1 was collected in a canyon which was part of a larger cave system of phreatic origin, preserved today as an assembly of cave

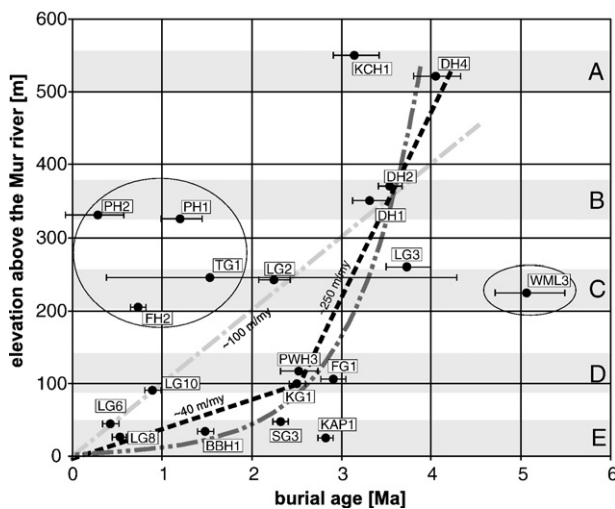


**Fig. 5.** Plot of burial age versus elevation above the Mur river. The data reveals the complex history of water table lowering related to valley entrenchment and aggradation. The speleogenetic levels are labeled as on Fig. 2. Trends are shown by dashed lines, an e-folding function is fitted through DH4, DH2, DH1, LG3, PWH3, FG1, KG1, SG3, BBH1; LG8, LG6 and the zero-point: elevation above Mur [m] =  $1.38 e^{1.58 \cdot \text{burial age [Ma]}}$  with a coefficient of determination  $R^2 = 0.58$ . Encircled samples are considered to not represent the age of the elevations they are situated in (see Section 3).

remnants in the Hochlantsch area, and related to the upper level of the Drachenhöhle (level A). This is the highest known occurrence of suitable cave sediments in the study area, so a sample was collected even though fieldwork indicated that later emplacement is possible.

The remaining data are all from caves where the stratigraphic relations between different cave sediments and the relationship between clastic sediments and passage morphology have given us confidence that there is no internal re-deposition from higher levels. The data are bracketed by the age of DH4 (Fig. 3C) from the upper level of the Drachenhöhle ( $4.05 \pm 0.28$  Ma at 968 m a.s.l., level A; sampled from a gravel bed known to be the stratigraphically oldest deposit within the passage; Schädler, 1931) and the current base level of the Mur River (at 440 m a.s.l. in the Hochlantsch region). This burial age suggests the onset of karstification to be earlier than 4 Ma, most likely already in the Miocene and permits using the remaining data set to compute a broad trend. A least square fit of the remaining data results in incision rates of  $\sim 90$  m/my, whereas the incision rate inferred only from DH4 and the current base level is  $\sim 130$  m/my; adding up to an average incision rate in the range of 100 m/my.

To determine deviations from this trend individual samples are discussed in more detail below. We begin with the samples from level B since level A is adequately discussed in the previous section. Based on the elevation correlation between the two study regions, the samples DH1 and DH2 from the lower level of the Drachenhöhle in the Hochlantsch area have their corresponding samples PH1 and PH2 in the Tanneben massif. Within the Drachenhöhle shafts ascend from the lower towards the upper level, but only one connecting passage is known. Remobilization of samples DH1 (Fig. 3F) and DH2 from the upper level is therefore unlikely. The  $\sim 3.4$  Ma of burial of these two samples indicates an incision rate of 270 m/my from level A to level B. The interpretation of the LG2 and LG3 ages is somewhat challenging, but they are the only meaningful samples from level C. Sample LG2 is from a wall notch (Fig. 3E) and LG3 from gravel cemented to the ceiling during an episode of in-filling. Both samples come from the upper level of the Lurgrotte not far from each other despite their obvious difference in age. LG2 ( $2.25 \pm 0.19$  Ma) is interpreted as being emplaced after the formation of the passage, whereas LG3 ( $3.73 \pm 0.27$  Ma) might indicate relocation from higher up; restricting the real age of passage formation to somewhere in between. Samples KG1, FG1 and PWH3 from level D consistently show burial ages between 2.5 and 2.9 Ma, and are well distributed all over the Tanneben massif. Field evidence and the consistent burial ages designate this level D to be a turning point: relatively rapid incision rates occurred prior to  $\sim 2.5$  Ma at  $\sim 250$  m/my and then decreased considerably to  $\sim 40$  m/my afterwards. LG10 (also from level D) was located below a one meter thick calcite false floor which is conserved as small remnants in the now further entrenched passage throughout level D in the Lurgrotte (Fig. 3G). This indicates a local aggradation event post-dating the original passage formation. SG3 is the only sample from the western side of the Mur valley and is located between levels D and E (Fig. 2). The cave from which sample SG3 was collected is one of 24 caves located in the center of one of the Mur rivers meanders and is related to an underground meander cutoff. The burial age is only somewhat younger than the samples from level D and the height difference of 60 m makes a continuing incision rate of 200 m/my down to this elevation plausible. Sample BBH1 comes from the only accessible horizontal phreatic cave (Fig. 3H) of the Schöckl area located south of the Tanneben massif (Fig. 1). Considering its position in the vicinity to the current base level it has a rather old burial age of  $1.48 \pm 0.09$  Ma. Potential re-deposition from higher levels could not be verified. Nevertheless the age fits well to the slow trend of the last 2–2.5 Ma. Finally, the active level E is most prominently developed in the active parts of the Lurgrotte cave system. Indeed, there is multiple evidence for young emplacement: (i) LG6 and LG8 have a consistent age of about 0.45 Ma despite their difference in elevation of 20 m (LG6 from an inactive sub-level). (ii) There are fine sediments interpreted to be the latest deposits of a damming event in close

proximity to sample LG6. We suggest that such damming may have occurred by blocking the cave outlet by sediment aggradation in the valley. (iii) Stalactites on this level often have gravels embedded in their tip (Fig. 3D). All this is evidence for incomplete passage fill related to such damming events. The burial ages might correlate to the Marine Isotope Stage (MIS) 12 and to related gravel aggradation (in classical Alpine terminology “Mindel”) in the Mur valley. An abandoned small cave in the Tanneben massif, the Kapellenhöhle, is the cave closest to the actual Mur river. From there sample KAP1 was successfully analyzed. Allochthonous consolidated gravels were recovered from the ceiling which consists of local collapse material and prevents further exploration. This suggests that the unexpectedly high burial age of  $2.82 \pm 0.09$  Ma of this deposit indicates re-mobilization from higher levels via conduits that are unknown and not, as we initially suspected, from a rather recent flood deposit, related to the event observed in the Lurgrotte just some hundreds of meters downstream.

In summary, we infer incision rates of the river Mur in the order of 100 m/my in the region 25 km upstream of the Alpine orogen–Pannonian basin transition at Graz during the last 4–5 my. Alternating phases of stability and pulses of incision successively created and abandoned cave levels. More detailed analysis of the data suggests that this incision was initially more rapid ( $\sim 250$  m/my) and slowed considerably (to about 40 m/my) towards the present.

#### 4. Discussion

Our determined mean incision rates are an order of magnitude lower than those from glacial valleys in the Swiss Alps obtained by the same method. However, they are in good agreement with rates prior to the influence of glacial carving (Häuselmann et al., 2007). Pre-burial erosion rates (around 20 m/my) show the same constancy over the evaluated time interval as data from Mammoth caves, Kentucky (Granger et al., 2001). That area is tectonically quite different, but of similar glacial setting as the region investigated here: It is also situated in a non-glaciated region in a marginal position to former ice-sheets. Even though glaciation is responsible for increased incision rates in the Mammoth Cave area, there is evidence of unchanged upland erosion rates throughout the investigated period of 3.5 my. Pre-burial erosion rates are slightly lower compared to our data from the orogen margin, which is interpreted to relate to the area's location in the interior low plateaus of the United States. Incision rates from burial ages of cave sediments in the Sierra Nevada mountains of California revealed similar rates of incision with the indication of decreasing rates towards present (Stock et al., 2004, 2005a) as is observed here. Possible scenarios capable of reducing rates of valley lowering are discussed below in the light of the geological setting of the study area, and are subsequently linked into an absolute vertical reference frame.

##### 4.1. Reduced incision during glaciation?

The decrease in incision rates since about 2.5 my is in contrast with increased erosion rates during this period as observed elsewhere in both the Alps and globally. Sediment budget data from the Eastern Alps (Kuhlemann et al., 2002, Kuhlemann, 2007) show an increase in rates at about the same time as the incision rate in the Mur valley decreased. In the glaciated regions of the Alps higher incision rates due to ice carving during glacial periods are well documented (e.g. Schlunegger and Hinderer, 2003) for part of the low-incision interval determined from our data. Caves of deeper levels may have formed during the interglacials, but the valley deepening itself occurred during glacial carving (Häuselmann et al., 2007). Molnar (2004) observed a worldwide increase in sedimentation rates around 2–4 Ma which is attributed to increased erosion rates due to climate oscillations.

We suggest that increased sediment discharge rates in most of the Alps in the last few million years provides a possible explanation for our observations of decreased incision rates in the non-glaciated part of the Alps. Sediments transported from the headwaters within that time period accumulated in the Mur valley and may have protected the bedrock from further incision. During such times, the river system is in a transport limited state – in contrast to the detachment limited state during bedrock incision stages (Whipple, 2004; Wobus et al., 2006). Only after the sediments have been eroded again, bedrock incision can continue. As such, there would be an oscillating scenario of valley aggradation and entrenchment in the Mur valley resulting in a decreased mean incision rate during the second half of our inferred evolution. Today, preserved last-glacial gravels prevent further bedrock incision in the Mur valley and are currently being excavated. A similar scenario is observed along the Drava river crossing the Pohorje dome. That region is similar as it was also not glaciated and fed by glaciated headwaters (as the source for sediment supply). There is also evidence for recent/ongoing uplift (Sölvä et al., 2005). Moreover the Mur and the Drava share the same base level and merge some 80 km downstream of Radkersburg. As there are no limestones and consequently no caves could form, an exposure age of  $14.75 \pm 1.7$  ka deduced from a quartz vein (D. Fabel, unpublished data) just above the current river level implies that there is currently no bedrock incision. If this can be assumed to be representative for the entire 2.5 my, it is feasible that bedrock incision is reduced in times of a transport limited state of a river system.

In view of this interpretation, it is important to note that there are other explanations for rivers being in a transport limited state (other than too much sediment from upstream sections). These include (i) too much sediment supply from the hillslopes by landslide or rockfall events during pulses of stronger incision, and (ii) decrease in stream power by decreasing catchment size or by decreasing river gradients (channel slopes). Because of the long duration of the decreased incision rate period, the first of these two alternatives is excluded. However, decreasing the stream power by changing the base level is conceivable for the Mur incision history: Uplift of the inverting Styrian Basin (Ebner and Sachsenhofer, 1995; Sachsenhofer et al., 1997) downstream of the study area may have lifted the local base level leading to a change from a detachment to a transport limited state. Also, the fact that the modeled pre-burial erosion rates are low (about 20% of the inferred average incision rate) indicates that the sampled gravels stem from source areas of continuous and slow erosion rates (Fig. 4B). Therefore, we suggest that the cave sediments cannot come from the glaciated region (where erosion rates are undoubtedly higher) and stem from local sources.

#### 4.2. Uplift or incision?

In order to infer aspects of the landscape evolution of the Alps, the incision history documented above needs to be placed into an absolute vertical reference frame. Two end member scenarios are possible: (a) no recent tectonic uplift occurred and the Mur dissected a topography of some 2000 m elevation with an over-steepened channel gradient at the orogen-basin transition near Graz, where it plummeted into the basin. (b) The Mur is an antecedent river at more or less constant elevation since 5 Ma with the incision history reflecting the surface uplift of the surrounding topography. Based on reasons outlined below, we suggest a scenario closer to the latter of these two possibilities.

The topographic history of the Styrian basin is reasonably well known (detailed review by Ebner and Sachsenhofer, 1995). The youngest marine sediments in the basin are shallow-water limestones of Upper Badenian age (~13 Ma), currently found at an altitude of ~400 m a.s.l. analogous to ~100 m above the present river bed some tens of kilometers downstream of the region considered here. Thereafter marine conditions ended and brackish to limnic conditions prevail in much of the basin. Important to note is a considerable hiatus in sediment record more pronounced in the Western than in the

Eastern Styrian basin, where Upper Badenian to Upper Pliocene sediments are truncated (Piller et al., 2004). This fact is interpreted to be the consequence of erosion due to uplift of the region (e.g. Ebner and Sachsenhofer, 1995; Sachsenhofer et al., 1997). This uplift is likely to be spatially broad, as gravel spreads do not show any substantial tilt or elevation differences between terraces of different age (Winkler-Hermaden, 1957). Exhumation in the surrounding Koralpe, Gleinalpe and Wechsel mountains is moderate or small, as apatite fission track ages preserve a much older stage of the exhumation history around 40–50 Ma (Hejl, 1997). Penetrations would not be preserved if erosion/exhumation would be high.

From these combined observations it is likely that the base level at the orogen-basin transition was around sea level up to about 8–5 Ma and then rose to its present elevation of some 350 m since then (presuming no sudden reversal/subsidence in the meantime), neglecting eustatic sea level changes. As the channel profile of the Mur shows no obvious knick point at the orogen-basin transition (Robl et al., 2008) and seismic activity is absent, an uplifting realm coupling basin and orogen is likely. Thus we suggest that most of our documented relative incision history reflects surface uplift of the study area.

This interpretation is supported by the capture history of the Mur river. Dunkl et al. (2005) suggested, based on apatite fission track age-provenance data, that it is only since the Mid-Miocene or later that today's course of the Mur river developed. Prior to this time, the river draining the upstream regions followed the Mur/Mürz fault system in an easterly direction and drained either through the Mürz valley into the Vienna basin and/or through the Lavant valley to the south (Dunkl et al., 2005; Fig. 1). In such a scenario, the Paleo-Mur near Graz would only have been a stream draining local areas. During a slight difference in surface uplift of the orogen relative to the basin, this stream would steepen and migrate headwards. This headward migration needs to cut only a distance of about 10 km of crystalline bedrock and a negligible vertical distance (Frisch et al., 1998) to reach Bruck. Thus, this headwards migrating river would eventually reach the Mur-Mürz fault system thereby capturing drainages from there and substantially increasing its catchment, causing the onset of rapid incision in the lower reaches of the system. This headward migration has been facilitated by the fact that the Noric Depression (the pull-apart basins along the Mur-Mürz fault) was once a consistent elongated basin with high sediment thickness (Frisch et al., 1998), which has been eroded since then. This is revealed by vitrinite reflectance data of coals from the basin fillings. It could be shown that paleo-sediment cover was substantial, especially in the basin of Leoben-Bruck (Sachsenhofer, 1989). This is exactly where the capture event happened. In addition the former more likely outlet of the Mur through the Lavant valley was uplifted in post-Middle Badenian times (Strauss et al., 2001).

The incision of about 500 m of bedrock within the last 4 Ma is consistent with the uplift history of the Styrian Basin a few kilometers downstream of the studied region. Based on vitrinite reflectance data and subsidence analysis, around 300–500 m of sediments have been eroded from the basin in the last ~5 Ma (Sachsenhofer et al., 1997, 2001). The increase in drainage area sometime after the Mid-Miocene due to stream capture resulted in a disequilibrium of incision rates of the trunk stream and its tributaries. As this might have happened not long before the investigated time, it could at least partly be reflected in the higher incision rates at the beginning of our investigated time span. That there was no general increase or decrease in local erosion rates over the investigated time span (concluded from the pre-burial erosion rate estimates of our data) suggests that there is no dramatic change in uplift rates in the source area of the cave sediments and no obvious climate change effect. The slow incision rates observed within the last ~2.5 Ma are closer to erosional steady state (geomorphologic decay) where values of incision rates and local erosion rates would be balanced. In other words, the two trends prior and after ~2.5 Ma both reflect rates of geomorphic disequilibrium.

These considerations suggest an intermediate scenario where increased erosional power due to enlargement of its catchment causes the river to dissect a slowly uplifting area. This increased stream power leads to effective entrenchment in the study area during the first ~1.5 my of the investigated time period. Thereafter, while adjusting to the new equilibrium state, the main river switches to a transport limited state due to decreasing river gradients but unchanged or even increasing sediment load. An increase in sediment load might be explained by overproduction of coarse sediment in the headwater regions related to glacial carving.

As the difference between incision rates before and after ~2.5 Ma is large, another possible scenario that would fit an e-folding function (as plotted in Fig. 5) would be a short-lived uplift pulse somewhere between 5 and 4 Ma, which slowed down thereafter. As there is strong evidence for the above discussed stream piracy event, a superposition of an uplift pulse and increase in drainage area is hard to separate. However, what argues against an uplift pulse is the fact that sediment budget of the Eastern Alps is not decreasing towards the present, but still increasing especially around 2 Ma where we see a decrease in incision rates (e.g. Kuhlemann, 2007).

Direct assessment of absolute surface uplift rates is not straight forward in this setting and we suspect uplift rates between the two incision trends, most likely around the mean rate of ~100 m/my. This implies a more gradual still ongoing – although not stable – uplift of the region. As this is the first data set of its kind it needs to be confirmed with additional investigations able to produce absolute rates of landscape evolution in time along the margin of the Eastern Alps.

Relating relative incision of the Mur river to surface uplift makes it necessary to touch upon the possible mechanisms that are responsible for this surface uplift. It seems reasonable to suggest the inversion of the Pannonian basin as the cause (Bada et al., 2007; Horváth and Cloething, 1996; Ruszkiczay-Rüdiger, 2007). In fact the actual renewal of dominance of north–south convergence is important (Fodor et al., 2005; Bus et al. 2009). Recent findings of vertical steps in the Moho in the region related to a possible Pannonian fragment which is underthrust by the European as well as the Adriatic plate (Brückl et al., 2007; Behm et al., 2007) arises the interest of possible mechanisms related to deeper seated processes. Slab break off or delamination have also been used to explain uplifting realms (e.g. Genser et al., 2007). Climate change alone has recently become attractive to explain increased uplift. Cederbom et al. (2004) suggested postorogenic mass reduction and isostatic rebound of the Swiss Alps and the neighboring foreland basin related to an increase in atmospheric moisture. The geomorphic setting in the study area allows us to exclude an important erosion-driven component to uplift, as pre-burial erosion rates of this study and fission track data (e.g. Hejl, 1997) contradicts such a setting.

## 5. Conclusion

In summary, we conclude the following points from the first successful burial age dating of cave sediments in the Eastern Alps, Austria:

- In the transition zone between Alpine orogen and Pannonian basin near Graz, the river Mur incised some 500 m in the last 4 my recording a very complex incision history resulting in a mean incision rate of about ~125 m/my. The karstification most likely started in late Miocene times (>4–5 my).
- Closer analysis of the data indicates higher incision rates (~250 m/my) prior to ~2.5 Ma followed by a considerable decrease in rates (~40 m/my) up to the present. The higher rates prior to ~2.5 Ma are related to surface uplift and an increase in catchment size as the result of stream piracy. The decrease in incision rate after ~2.5 Ma can be related to a shift from detachment limited to transport limited channel erosion of the main (Mur) river due to decreasing stream gradient and ample sediment supply from upstream

sections. A primarily climatic trigger for incision rate changes over time is unlikely because of constant pre-burial erosion rates over the whole time period. This fact also constrains changes of uplift of the local source area to be low.

- When put into a vertical reference frame, the relative incision rates allow us to infer rates of surface uplift in the order of 100 m/my. A detailed trend is not derivable, as stream piracy and later aggradation due to overproduction of coarse sediment in the headwater regions complicate the interpretation of the relative incision rates; although we exclude a short-lived uplift pulse. However, our data document the rejuvenation of a landscape that resided at low elevations during most of the Miocene over the last ~4 my.
- The cause of the uplift remains unsolved, but strong influence of the inversion of the Pannonian basin and the general change in the stress regime resulting in renewed north–south compression is likely.

## Acknowledgements

The authors thank the numerous cavers for sharing their knowledge and for discussions about the area. Special thanks to R. Benischke, H. Grillhofer, H. Kusch and S. Oswald, as well as the local caving clubs: Höhlenbären and the Landesverein für Höhlenkunde in der Steiermark. Without all of them such a study would have been impossible. L. Plan, M. Filipponi and C. Spötl are thanked for thought-provoking discussions and comments on this paper. Comments from Ari Matmon and one anonymous reviewer helped to improve the manuscript. We express our gratitude to John Hellstrom, University of Melbourne, for U–Th dating of the speleothems. Many thanks to Wilfried Körner for providing the ICP-OES data. Sincere thanks are given to E. Tillmanns and H. Effenberger (Institute of Mineralogy and Crystallography, Univ. Vienna) for their support of our laboratory work and to the Center of Earth Sciences for supporting our work in the frame of the Earth Science Cooperation between the University of Vienna and the University of Natural Resources and Applied Life Sciences, Vienna.

We greatly acknowledge the work of the SUERC AMS group in Glasgow, Scotland. The project was funded by the “Kooperationsprojekt Erdwissenschaften NAWI Graz (§ 141)” and the ESF project I-152.

## References

- Audra, Ph., Bini, A., Gabrovsek, F., Häuselmann, Ph., Hóbléa, F., Jeannin, P.-Y., Kunaver, J., Monbaron, M., Sustersic, F., Tognini, P., Trimmel, H., Wildberger, A., 2006. Cave genesis in the Alps between the Miocene and today: a review. *Z. Geomorph. N.F.* 50 (2), 153–176.
- Bada, G., Horváth, F., Dövényi, P., Szafián, P., Windhoffer, G., Cloething, S., 2007. Present-day stress field and tectonic inversion in the Pannonian basin. *Global Planet. Change* 58, 165–180.
- Behm, M., Brückl, E., Chwatal, W., Thybo, H., 2007. Application of stacking and inversion techniques to three-dimensional wide-angle reflection and refraction seismic data of the Eastern Alps. *Geophys. J. Int.* 170, 275–298.
- von Blanckenburg, F., 2005. The control mechanisms of erosion and weathering at basin scale from cosmogenic nuclides in river sediment. *Earth Planet. Sci. Lett.* 237, 462–479.
- Brückl, E., Bleibinhaus, F., Gosar, A., Grad, M., Guterch, A., Hrubcová, P., Keller, G.R., Majdanski, M., Sumanovac, F., Tiira, T., Yliniemi, J., Hegedüs, E., Thybo, H., 2007. Crustal structure due to collisional and escape tectonics in the Eastern Alps region based on profiles Alp01 and Alp02 from the ALP 2002 seismic experiment. *J. Geophys. Res.* 112, B06308. doi:10.1029/2006JB004687.
- Bus, Z., Grenczy, Gy, Tóth, L., Mónus, P., 2009. Active crustal deformation in two seismogenic zones of the Pannonian region – GPS versus seismological observations. *Tectonophysics* 474, 343–352.
- Cederbom, C.E., Sinclair, H.D., Schlunegger, F., Rahn, M.K., 2004. Climate-induced rebound and exhumation of the European Alps. *Geology* 32, 709–712.
- Champagnac, J.D., Schlunegger, F., Norton, K., von Blanckenburg, F., Abbühl, L.M., Schwab, M., 2009. Erosion-driven uplift of the modern Central Alps. *Tectonophysics* 474, 236–249.
- Dunkl, I., Frisch, W., 2002. Thermochronological constraints on the Late Cenozoic exhumation along the Alpine and West Carpathian margins of the Pannonian basin. *EGU Stephan Mueller Special Publication Series* 3, 135–147.
- Dunkl, I., Kuhlemann, J., Reinecker, J., Frisch, W., 2005. Cenozoic relief evolution of the Eastern Alps – constraints from apatite fission track age-provenance of neogene intramontane sediments. *Aust. J. Earth Sci.* 98, 92–105.

- Ebner, F., Sachsenhofer, R.F., 1995. Paleogeography, subsidence and thermal history of the Neogene Styrian Basin (Pannonian basin system, Austria). *Tectonophysics* 242, 133–150.
- Fodor, L., Bada, G., Csillag, G., Horváth, E., Ruszkiczay-Rüdiger, Zs., Palotás, K., Síkhegyi, F., Timár, G., Cloetingh, S., Horváth, F., 2005. An outline of neotectonic structures and morphotectonics of the western and central Pannonian Basin. *Tectonophysics* 410, 15–41.
- Frisch, W., Kuhlemann, J., Dunkl, I., Brügel, A., 1998. Palinspastic reconstruction and topographic evolution of the Eastern Alps during late Tertiary tectonic extrusion. *Tectonophysics* 297, 1–15.
- Frisch, W., Kuhlemann, J., Dunkl, I., Szekely, B., 2001. The Dachstein paleosurface and the Augenstein Formation in the Northern Calcareous Alps; a mosaic stone in the geomorphological evolution of the Eastern Alps. *Int. J. Earth Sci.* 90, 500–518.
- Gasser, D., Stüwe, K., Fritz, H., 2009. Internal structural geometry of the Paleozoic of Graz. *Int. J. Earth Sci.* doi:10.1007/s00531-009-0446-0.
- Genser, J., Cloetingh, S., Neubauer, F., 2007. Late orogenic rebound and oblique Alpine convergence: New constraints from subsidence analysis of the Austrian Molasse basin. *Global Planet. Change* 58, 214–223.
- Gosse, J.C., Phillips, F.M., 2001. Terrestrial in situ cosmogenic nuclides: theory and application. *Quat. Sci. Rev.* 20, 1475–1560.
- Granger, D.E., Fabel, D., Palmer, A.N., 2001. Pliocene–Pleistocene incision of the Green River, Kentucky, determined from radioactive decay of cosmogenic <sup>26</sup>Al and <sup>10</sup>Be in Mammoth Cave sediments. *Geol. Soc. Am. Bull.* 113, 825–836.
- Granger, D.E., Muzikar, P.F., 2001. Dating sediment burial with in situ-produced cosmogenic nuclides: theory, techniques, and limitations. *Earth Planet. Sci. Lett.* 188, 269–281.
- Grencz, G., Kenyeres, A., Fejes, I., 2000. Present crustal movement and strain distribution in Central Europe inferred from GPS measurements. *J. Geophys. Res.* 105, 21835–21846.
- Grencz, G., Sella, G., Stein, S., Kenyeres, A., 2005. Tectonic implications of the GPS velocity field in the northern Adriatic region. *Geophys. Res. Lett.* 32, L16311. doi:10.1029/2005GL022947.
- Häuselmann, Ph., Granger, D.E., 2005. Dating of caves by cosmogenic nuclides: method, possibilities, and the Siebenhengste example (Switzerland). *Acta Carsologica* 34 (1), 43–50.
- Häuselmann, Ph., Granger, D.E., Jeannin, P.-Y., Lauritzen, S.-E., 2007. Abrupt glacial valley incision at 0.8 Ma dated from cave deposits in Switzerland. *Geology* 35, 143–146.
- Hejl, E., 1997. 'Cold spots' during the Cenozoic evolution of the Eastern Alps: thermo-chronological interpretation of apatite fission-track data. *Tectonophysics* 272, 159–173.
- Hellstrom, J., 2003. Rapid and accurate U/Th dating using parallel ion-counting multi-collector ICP-MS. *J. Anal. At. Spectrom.* 18, 1346–1351.
- Hellstrom, J., 2006. U–Th dating of speleothems with high initial <sup>230</sup>Th using stratigraphical constraint. *Quatern. Geochronol.* 1, 289–295.
- Horváth, F., Cloetingh, S., 1996. Stress-induced late-stage subsidence anomalies in the Pannonian basin. *Tectonophysics* 266, 287–300.
- Kahle, H.G., et al., 1997. Recent crustal movements, geoid and density distribution: contribution from integrated satellite and terrestrial measurements. In: Pfiffner, O. A., Lehner, P., Heitzmann, P., Müller, St., Steck, A. (Eds.), *Results of the National Research Program 20 (NRP 20)*. Birkhäuser, Basel, pp. 251–259.
- Kuhlemann, J., Frisch, W., Szekely, B., Dunkl, I., Kazmer, M., 2002. Post-collisional sediment budget history of the Alps: Tectonic versus climatic control. *Int. J. Earth Sci.* 91, 818–837.
- Kuhlemann, J., 2007. Paleogeographic and paleotopographic evolution of the Swiss and Eastern Alps since the Oligocene. *Global Planet. Change* 58, 224–236.
- Luth, S.W., Willingshofer, E., 2008. Mapping of the post-collisional cooling history of the Eastern Alps. *Swiss J. Geosci.* 101, Supplement 1, 207–223.
- Maurin, V., Benischke, R., 1992. Morphogeny, Paleohydrography and Karst Development, in: H. Behrens et al., *Investigations with Natural and Artificial Tracers in the Karst Aquifer of the Lurbach System (Peggau–Tanneben–Semriach, Austria)*. *Steir. Beitr. z. Hydrogeologie* 43, 22–33.
- Molnar, P., 2004. Late Cenozoic increase in accumulation rates of terrestrial sediment: how might climate change have affected erosion rates? *Annu. Rev. Earth Planet. Sci.* 32, 76–89.
- Nishiizumi, K., Winterer, E.L., Kohl, C.P., Klein, J., Middleton, R., Lal, D., Arnold, J.R., 1989. Cosmic ray production rates of <sup>10</sup>Be and <sup>26</sup>Al in quartz from glacially polished rocks. *J. Geophys. Res.* 94, 17907–17915.
- Norton, K.P., von Blanckenburg, F., Kubik, P.W., 2010. Cosmogenic nuclide-derived rates of diffusive and episodic erosion in the glacially sculpted upper Rhone Valley, Swiss Alps. *Earth Surf. Process. Land.* doi:10.1002/esp.1961.
- Palmer, A.N., 1987. Cave levels and their interpretation. *NSS Bulletin* 49, 50–66.
- Piller, W.E., Egger, H., Erhart, C.W., Gross, M., Harzhauser, M., Hubmann, B., Vav Husen, D., Krenmayr, H.-G., Krystyn, L., Lein, R., Lukeneder, A., Mandl, G.W., Rögl, F., Roetzel, R., Rupp, C., Schnabel, W., Schönlaub, H.P., Summesberger, H., Wagreich, M. and Wesseley, G., 2004. Die stratigraphische Tabelle von Österreich 2004 (sedimentäre Folgen). *Komm. paläont. stratigr. Erforsch. Österr., Österr. Akad. Wiss. und Österr. Stratigr. Komm.*, Wien.
- Ratschbacher, L., Frisch, W., Linzer, H.-G., Merle, O., 1991. Lateral extrusion in the Eastern Alps 2. Structural analysis. *Tectonics* 10, 257–271.
- Robl, J., Hergarten, S., Stüwe, K., 2008. Morphological analysis of the drainage system in the Eastern Alps. *Tectonophysics* 460, 263–277.
- Ruess, D., Höggerl, N., 2002. Bestimmung rezenter Höhen- und Schwereänderungen in Österreich. In: Friedl, G., Genser, J., Handler, R., Neubauer, F., Steyrer, H.-P. (Eds.), *Pangeo Austria*. Institut für Geologie und Paläontologie. Universität Salzburg, Salzburg, p. 151.
- Ruszkiczay-Rüdiger, Zs., 2007. Tectonic and climatic forcing in Quaternary landscape evolution in the Central Pannonian Basin: A quantitative geomorphological, geochronological and structural analysis. PhD Thesis, Vrije Universiteit, Amsterdam, Netherlands.
- Sachsenhofer, R.F., 1989. Das Inkohlungs bild im Jungtertiär der Norischen Senke (Östliche Zentralalpen, Österreich) und seine paläogeothermische Deutung. *Jb. Geol. B.-A.* 132 (2), 489–505.
- Sachsenhofer, R.F., Lankreier, A., Cloetingh, S., Ebner, F., 1997. Subsidence analysis and quantitative basin modelling in the Styrian Basin (Pannonian Basin System, Austria), in: Neubauer, F., Cloetingh, S., Dinu, C. and Mocanu, V. (Eds.), *Tectonics of the Alpine–Carpathian–Pannonian Region. II* *Tectonophysics* 272, 175–196.
- Sachsenhofer, R.F., Jelen, B., Hasenhüttl, C., Dunkl, I., Rainer, T., 2001. Thermal history of Tertiary basins in Slovenia (Alpine–Dinaride–Pannonian junction). *Tectonophysics* 334, 77–99.
- Schadler, J., 1931. Die Ablagerungen. In: Abel, O., Kyrle, G. (Eds.), *Die Drachenhöhle bei Mixnitz. Speleologische Monographien*, 7–8, pp. 169–224.
- Schlunegger, F., Hinderer, M., 2001. Crustal uplift in the Alps – why the drainage pattern matters. *Terra Nova* 13, 425–432.
- Schlunegger, F., Hinderer, M., 2003. Pleistocene/Holocene climate change, re-establishment of fluvial drainage network and increase in relief in the Swiss Alps. *Terra Nova* 15, 88–95.
- Sölva, H., Stüwe, K., Strauss, P., 2005. The Drava River and the Pohorje Mountain Range (Slovenia): geomorphological interactions. *Mitt. d. Naturwissenschaftlichen V. für Stmk.* 134, 45–55.
- Stock, G.M., Anderson, R.S., Finkel, R.C., 2004. Pace of landscape evolution in the Sierra Nevada, California, revealed by cosmogenic dating of cave sediments. *Geology* 32, 193–196.
- Stock, G.M., Granger, D.E., Sasowsky, I.D., Anderson, R.S., Finkel, R.C., 2005a. Comparison of U–Th, paleomagnetism, and cosmogenic burial methods for dating caves: implications for landscape evolution studies. *Earth Planet. Sci. Lett.* 236, 388–403.
- Stock, G.M., Anderson, R.S., Finkel, R.C., 2005b. Rates of erosion and topographic evolution of the Sierra Nevada, California, inferred from cosmogenic <sup>26</sup>Al and <sup>10</sup>Be concentrations. *Earth Surf. Process. Landforms* 30, 985–1006.
- Strauss, P., Wagreich, M., Decker, K., Sachsenhofer, R.F., 2001. Tectonics and sedimentation in the Fohnsdorf–Seckau Basin (Miocene, Austria): from pull-apart basin to a half-graben. *Int. J. Earth Sci.* 90, 549–559.
- Székely, B., Reinecker, J., Dunkl, I., Frisch, W., Kuhlemann, J., 2002. Neotectonic movements and their geomorphic response as reflected in surface parameters and stress patterns in the Eastern Alps. *EGU Stephan Mueller Special Publication Series* 3, 149–166.
- Van Husen, D., 1999. Geological processes during the Quaternary. *Mitt. Oesterr. Geol. Ges.* 92, 135–156.
- Vernon, A.J., van der Beek, P.A., Sinclair, H.D., Rahn, M.K., 2008. Increase in late Neogene denudation of the European Alps confirmed by analysis of a fission-track thermochronology database. *Earth Planet. Sci. Lett.* 270, 316–329.
- Whipple, K.X., 2004. Bedrock rivers and the geomorphology of active orogens. *Annu. Rev. Earth Planet. Sci.* 32, 151–185.
- Winkler-Hermaden, A., 1955. Ergebnisse und Probleme der quartären Entwicklungsgeschichte am östlichen Alpensaum außerhalb der Vereisungsgebiete. *Denkschr. Akad. Wiss. math.-naturw. Kl.*, 110, Wien.
- Winkler-Hermaden, A., 1957. *Geologisches Kräftespiel und Landformung*. Springer Verlag, Wien, p. 822.
- Wittmann, H., von Blanckenburg, F., Kruesmann, T., Norton, K.P., Kubik, P.W., 2007. Relation between rock uplift and denudation from cosmogenic nuclides in river sediment in the Central Alps of Switzerland. *J. Geophys. Res.* Earth Surf. 112.
- Wobus, C., Whipple, K.X., Kirby, E., Snyder, N., Johnson, J., Spyropoulou, K., Crosby, B., Sheeha, D., 2006. Tectonics from topography: Procedures, promises, and pitfalls, in: Willet, S.D., Hovius, N., Brandon, M.T., Fisher, D.M., (Eds.), *Tectonics, Climate, and Landscape Evolution. Spec. Pap. Geol. Soc. Am.* 398, 55–74.